Long-lived particle searches at future colliders

Nivedita Ghosh
Presented in Phoenix

19^{th} December, 2023

Outline

Based on the work:
Light long-lived particles at the FCC-hh with the proposal for a dedicated forward detector FOREHUNT and a transverse detector DELIGHT (Arxiv: 2306.11803),Biplob Bhattacherjee, Herbi K. Dreiner, **NG**, Shigeki Matsumoto, Rhitaja Sengupta, Prabhat Solanki

Motivation

- Long-lived BSM particles (LLPs) ($c\tau \gtrsim \mathcal{O}(\mathrm{mm})$).

[1] Kling et al, Phys. Rev. D 97 (2018) 035001
[2] Curtin et al, Phys. Rev. D 98 (2018) 115005
[3] Aielli et al., Eur. Phys. J. C 80 (2020) 1177
[4] Bauer et al., 1909.13022

Motivation

- Long-lived BSM particles (LLPs) ($c\tau \gtrsim \mathcal{O}(\mathrm{mm})$).
- The CMS and ATLAS detectors extend up to $\mathcal{O}$ (10 m).

[1] Kling et al, Phys. Rev. D 97 (2018) 035001
[2] Curtin et al, Phys. Rev. D 98 (2018) 115005
[3] Aielli et al., Eur. Phys. J. C 80 (2020) 1177
[4] Bauer et al., 1909.13022

Motivation

- Long-lived BSM particles (LLPs) ($c\tau \gtrsim \mathcal{O}(\mathrm{mm})$).
- The CMS and ATLAS detectors extend up to $\mathcal{O}$ (10 m).
- Light LLPs with large decay lengths are more likely to decay outside the LHC main detector volumes due to the high boost values $\rightarrow$ Dedicated detectors needed.

[1] Kling et al, Phys. Rev. D 97 (2018) 035001
[2] Curtin et al, Phys. Rev. D 98 (2018) 115005
[3] Aielli et al., Eur. Phys. J. C 80 (2020) 1177
[4] Bauer et al., 1909.13022

Motivation

- Long-lived BSM particles (LLPs) ($c\tau \gtrsim \mathcal{O}(\mathrm{mm})$).
- The CMS and ATLAS detectors extend up to $\mathcal{O}$ (10 m).
- Light LLPs with large decay lengths are more likely to decay outside the LHC main detector volumes due to the high boost values → Dedicated detectors needed.
- Depending on the production mode, LLP can traverse either in forward or transverse direction.

[1] Kling et al, Phys. Rev. D 97 (2018) 035001
[2] Curtin et al, Phys. Rev. D 98 (2018) 115005
[3] Aielli et al., Eur. Phys. J. C 80 (2020) 1177
[4] Bauer et al., 1909.13022

Motivation

- Long-lived BSM particles (LLPs) ($c\tau \gtrsim \mathcal{O}(\mathrm{mm})$).
- The CMS and ATLAS detectors extend up to $\mathcal{O}$ (10 m).
- Light LLPs with large decay lengths are more likely to decay outside the LHC main detector volumes due to the high boost values $\rightarrow$ Dedicated detectors needed.
- Depending on the production mode, LLP can traverse either in forward or transverse direction.
- At LHC, FASER (ForwArd Search ExpeRiment) [1] is one such detector specifically designed to look for light LLPs in the far forward region while there are proposed experiments in the transverse direction, like MATHUSLA [2], CODEX-b [3], and ANUBIS [4].

[1] Kling et al, Phys. Rev. D 97 (2018) 035001
[2] Curtin et al, Phys. Rev. D 98 (2018) 115005
[3] Aielli et al., Eur. Phys. J. C 80 (2020) 1177
[4] Bauer et al., 1909.13022

Motivation

- Long-lived BSM particles (LLPs) ($c\tau \gtrsim \mathcal{O}(\mathrm{mm})$).
- The CMS and ATLAS detectors extend up to $\mathcal{O}$ (10 m).
- Light LLPs with large decay lengths are more likely to decay outside the LHC main detector volumes due to the high boost values $\rightarrow$ Dedicated detectors needed.
- Depending on the production mode, LLP can traverse either in forward or transverse direction.
- At LHC, FASER (ForwArd Search ExpeRiment) [1] is one such detector specifically designed to look for light LLPs in the far forward region while there are proposed experiments in the transverse direction, like MATHUSLA [2], CODEX-b [3], and ANUBIS [4].
- **Not any proposal for 100 TeV FCC-hh !!**

[1] Kling et al, Phys. Rev. D 97 (2018) 035001
[2] Curtin et al, Phys. Rev. D 98 (2018) 115005
[3] Aielli et al., Eur. Phys. J. C 80 (2020) 1177
[4] Bauer et al., 1909.13022

Dark Higgs Scalar

The Lagrangian can be written as [5]

$$\mathcal{L} = \mathcal{L}_{\rm SM} + \mu_\Phi^2 \Phi^2 - \frac{1}{4}\lambda_\Phi \Phi^4 - \epsilon \Phi^2 |H|^2 \,. \qquad (1)$$

[5] Li et al, Arxiv:2212.06186

Dark Higgs Scalar

The Lagrangian can be written as [5]

$$\mathcal{L} = \mathcal{L}_{\rm SM} + \mu_\Phi^2 \Phi^2 - \frac{1}{4}\lambda_\Phi \Phi^4 - \epsilon \Phi^2 |H|^2 \,. \tag{1}$$

$$\begin{aligned} h_{125} &= \Phi \sin\theta + h \cos\theta \,, \\ \phi &= \Phi \cos\theta - h \sin\theta, \end{aligned} \tag{2}$$

[5] Li et al, Arxiv:2212.06186

Dark Higgs Scalar

The Lagrangian can be written as [5]

$$\mathcal{L} = \mathcal{L}_{\rm SM} + \mu_\Phi^2 \Phi^2 - \frac{1}{4}\lambda_\Phi \Phi^4 - \epsilon \Phi^2 |H|^2 \,. \tag{1}$$

$$\begin{aligned} h_{125} &= \Phi \sin\theta + h\cos\theta \,, \\ \phi &= \Phi\cos\theta - h\sin\theta, \end{aligned} \tag{2}$$

$$\mathcal{L}_{\rm int} = \phi \sin\theta \sum_f \frac{m_f}{v} \bar{f} f \,, \tag{3}$$

[5] Li et al, Arxiv:2212.06186

Dark Higgs Scalar

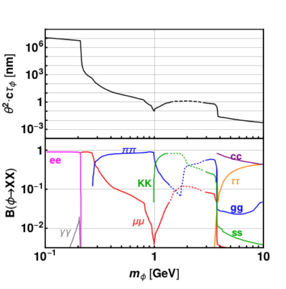

$$\Gamma_{\phi \to f\bar{f}} = \frac{N_c G_F m_\phi m_f^2 \sin^2\theta}{4\sqrt{2}\pi} \left(1 - \frac{4m_f^2}{m_\phi^2}\right)^{3/2} \tag{4}$$

Dark Higgs Scalar

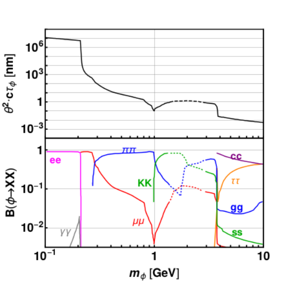

$$\Gamma_{\phi \to f\bar{f}} = \frac{N_c G_F m_\phi m_f^2 \sin^2\theta}{4\sqrt{2}\pi} \left(1 - \frac{4m_f^2}{m_\phi^2}\right)^{3/2} \quad (4)$$

If the mixing angle, $\sin\theta$, is very small, the proper decay length of the dark Higgs scalar is $c\tau \sim$ few mm, making the particle long-lived.

Dark Higgs Scalar

ϕ to be very light, with its mass ranging from $\sim 100\,\text{MeV}$ to few GeV.

[6] FASER collaboration, PhysRevD.99.095011

Dark Higgs Scalar

ϕ to be very light, with its mass ranging from $\sim 100\,\text{MeV}$ to few GeV.
$B^{\pm} \to K^{\pm}\phi$ [6]

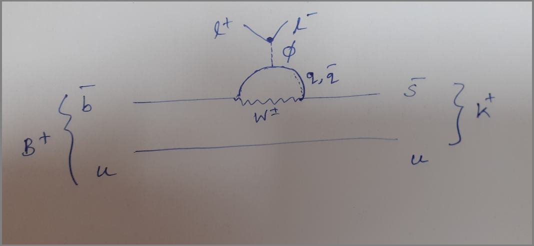

$$\mathcal{B}r(B^{\pm} \to K^{\pm}\phi) \approx 5.7 \sin^2\theta \left(1 - \frac{m_\phi^2}{m_b^2}\right)^2 \quad (5)$$

where $m_B = 5.28$ GeV, $m_K = 0.494$ GeV, and $m_b = 4.75$ GeV .

[6] FASER collaboration, PhysRevD.99.095011

Analysis Setup

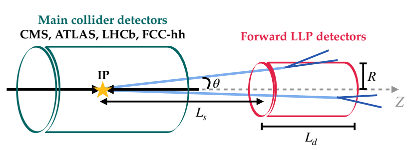

FASER R 10 cm and ,L_d 1.5 m, placed at 480 m in the z-axis from the IP, aiming to collect data during LHC run3 2021-2023 [7] for integrated luminosity 150 fb^{-1}.

[7] FASER collaboration, Phys. Rev. D 99 (2019) 095011

Analysis Setup

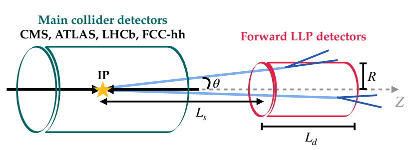

FASER R 10 cm and ,L_d 1.5 m, placed at 480 m in the z-axis from the IP, aiming to collect data during LHC run3 2021-2023 [7] for integrated luminosity 150 fb^{-1}.
FASER2 will possess a radius of 1 m and a length of 5 m, and it is expected to collect data for HL-LHC in the era 2026-2035 with an integrated luminosity of $\mathcal{L} = 3000\ \mathrm{fb}^{-1}$.

[7] FASER collaboration, Phys. Rev. D 99 (2019) 095011

Analysis Setup

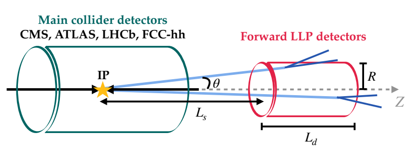

FASER R 10 cm and ,L_d 1.5 m, placed at 480 m in the z-axis from the IP, aiming to collect data during LHC run3 2021-2023 [7] for integrated luminosity 150 fb^{-1}.
FASER2 will possess a radius of 1 m and a length of 5 m, and it is expected to collect data for HL-LHC in the era 2026-2035 with an integrated luminosity of $\mathcal{L} = 3000\ \mathrm{fb}^{-1}$.

$$P_{\rm decay} = \frac{(1 - e^{\frac{-L_1}{|D_z|}})}{e^{\frac{L_s}{|D_z|}}}\,, \tag{6}$$

where $D_z = \frac{p_z}{m} c\tau$.

[7] FASER collaboration, Phys. Rev. D 99 (2019) 095011

Analysis Setup

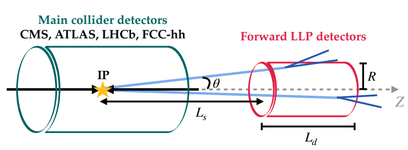

FASER R 10 cm and ,L_d 1.5 m, placed at 480 m in the z-axis from the IP, aiming to collect data during LHC run3 2021-2023 [7] for integrated luminosity 150 fb^{-1}.
FASER2 will possess a radius of 1 m and a length of 5 m, and it is expected to collect data for HL-LHC in the era 2026-2035 with an integrated luminosity of $\mathcal{L} = 3000\ \mathrm{fb}^{-1}$.

$$P_{\rm decay} = \frac{(1 - e^{\frac{-L_1}{|D_z|}})}{e^{\frac{L_s}{|D_z|}}}\,, \tag{6}$$

where $D_z = \frac{p_z}{m} c\tau$.

$$\epsilon_{\rm LLP} = \frac{\sum_i P^i_{\rm decay}}{N_{\rm events}}\,, \tag{7}$$

[7] FASER collaboration, Phys. Rev. D 99 (2019) 095011

Analysis Setup

$$N_{\text{detector}} = \sigma_{bb} \times \epsilon_{B^{\pm}} \times \mathcal{B}r(B^{\pm} \rightarrow K^{\pm}\phi) \times \epsilon_{\text{LLP}} \times \mathcal{L} \tag{8}$$

$\sigma_{bb} = 9.4 \times 10^{11}\text{fb}$[8]
LLP decays to the visible particles with 100% branching ratio and will be detected in the detector only if the momentum $p_{\phi} > 100\,\text{GeV}$

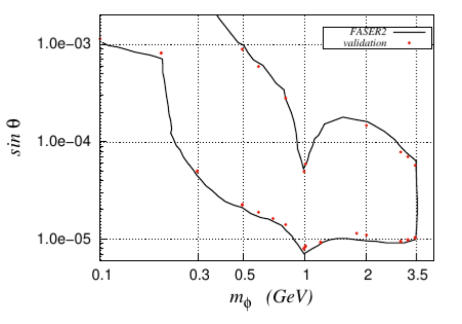

[8] validation done with FORESEE package, Kling et al

Why 100 TeV?

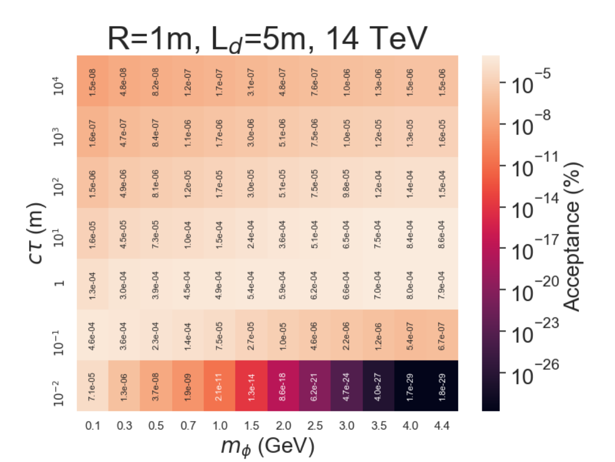

R=1m, L_d=5m, 14 TeV
cτ (m)
10^4
10^3
10^2
10^1
1
10^−1
10^−2
1.5e-08 4.8e-08 8.2e-08 1.2e-07 1.7e-07 3.1e-07 4.8e-07 7.6e-07 1.0e-06 1.3e-06 1.5e-06 1.5e-06
1.6e-07 4.7e-07 8.4e-07 1.1e-06 1.7e-06 3.0e-06 5.1e-06 7.5e-06 1.0e-05 1.2e-05 1.3e-05 1.6e-05
1.5e-06 4.9e-06 8.1e-06 1.2e-05 1.7e-05 3.0e-05 5.1e-05 7.5e-05 9.8e-05 1.2e-04 1.4e-04 1.5e-04
1.6e-05 4.5e-05 7.3e-05 1.0e-04 1.5e-04 2.4e-04 3.6e-04 5.1e-04 6.5e-04 7.5e-04 8.4e-04 8.6e-04
1.3e-04 3.0e-04 3.9e-04 4.5e-04 4.9e-04 5.4e-04 5.9e-04 6.2e-04 6.6e-04 7.0e-04 8.0e-04 7.9e-04
4.6e-04 3.6e-04 2.3e-04 1.4e-04 7.5e-05 2.7e-05 1.0e-05 4.6e-06 2.2e-06 1.2e-06 5.4e-07 6.7e-07
7.1e-05 1.3e-06 3.7e-08 1.9e-09 2.1e-11 1.3e-14 8.6e-18 6.2e-21 4.7e-24 4.0e-27 1.7e-29 1.8e-29
0.1 0.3 0.5 0.7 1.0 1.5 2.0 2.5 3.0 3.5 4.0 4.4
m_ϕ (GeV)
10^−5
10^−8
10^−11
10^−14
10^−17
10^−20
10^−23
10^−26
Acceptance (%)

Why 100 TeV?

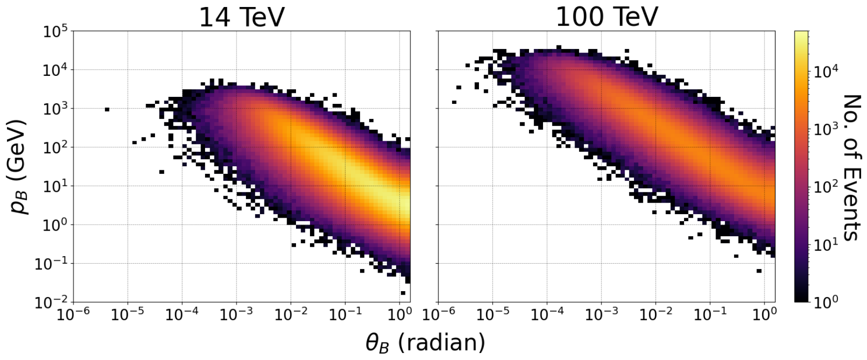

Why 100 TeV?

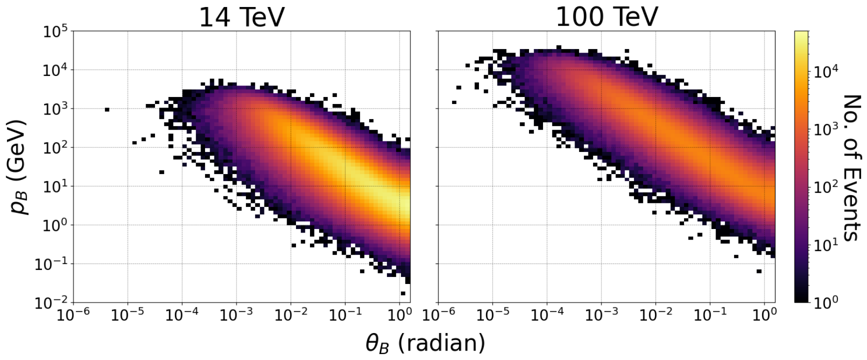

Compared to 14 TeV, at 100 TeV, the $B-$ mesons are much more forward.

Why 100 TeV?

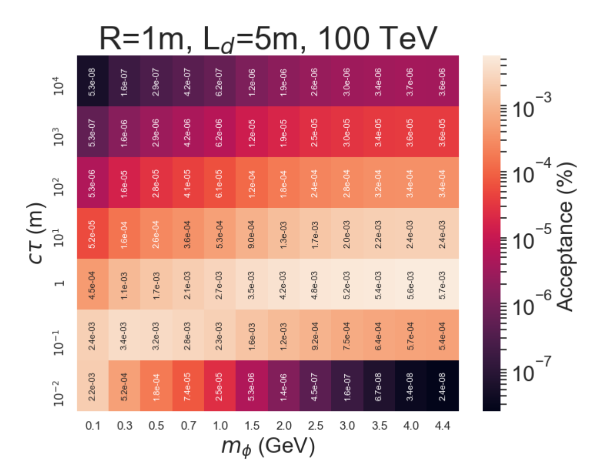

[9] Aleksa el at.,CERN-2022-002

Why 100 TeV?

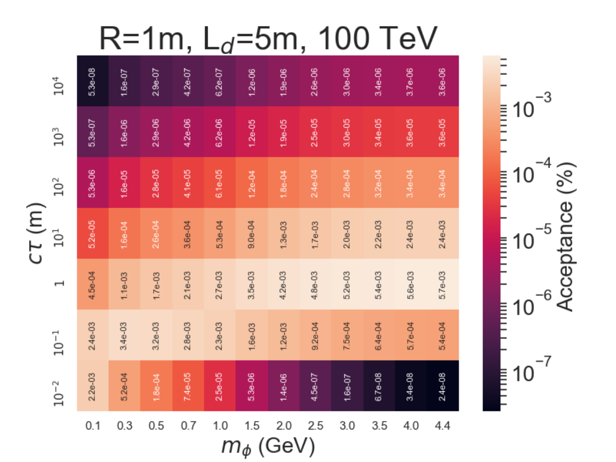

At future colliders like LHC at 100 TeV, we are not limited by the space constraint [9]

[9] Aleksa el at.,CERN-2022-002

Optimizing the detector

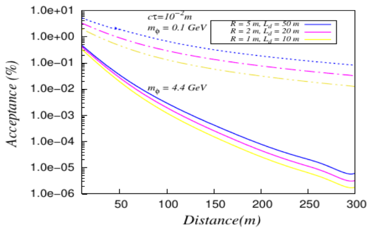

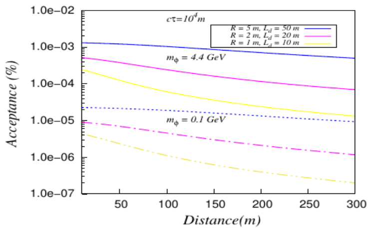

Optimizing the detector

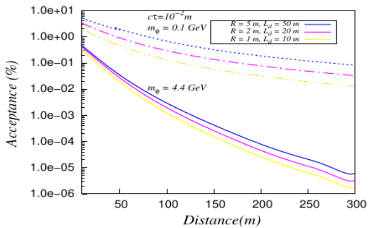

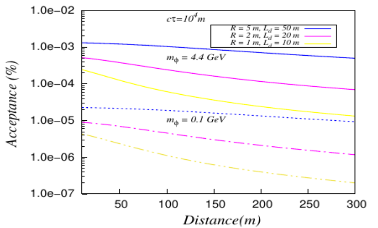

FOREHUNT(FORward Experiment for HUNdred TeV)

Optimizing the detector

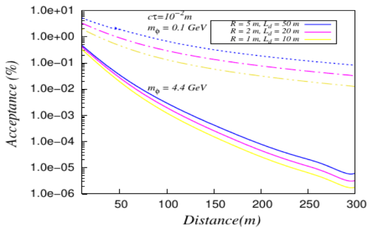

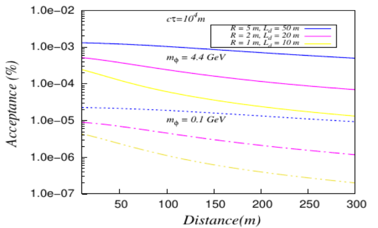

FOREHUNT(FORward Experiment for HUNdred TeV)

Detector Configuration @100 TeV	Radius (R)	Length (L_d)	Position (Z)
FOREHUNT-A	1 m	10 m	50 m
FOREHUNT-B	2 m	20 m	50 m
FOREHUNT-C	5 m	50 m	50 m
FOREHUNT-D	2 m	20 m	75 m
FOREHUNT-E	5 m	50 m	75 m
FOREHUNT-F	5 m	50 m	100 m

Optimizing the detector

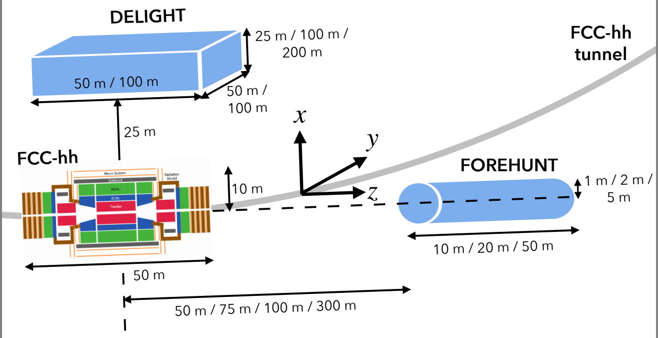

Dark Higgs

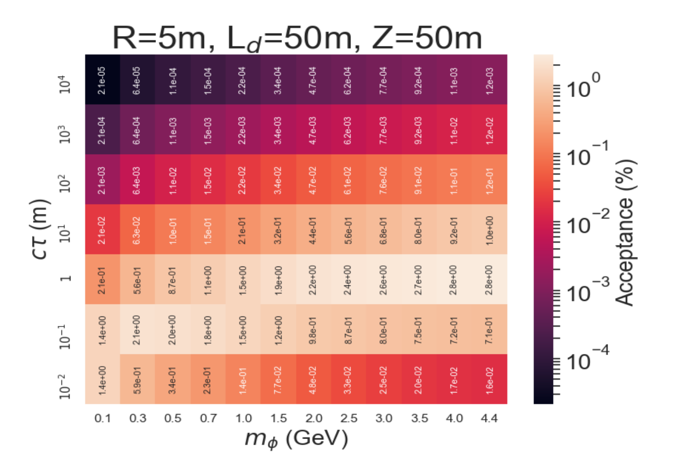

R=5m, L$_d$=50m, Z=50m
$c\tau$ (m)
10^4 2.1e-05 6.4e-05 1.1e-04 1.5e-04 2.2e-04 3.4e-04 4.7e-04 6.2e-04 7.7e-04 9.2e-04 1.1e-03 1.2e-03
10^3 2.1e-04 6.4e-04 1.1e-03 1.5e-03 2.2e-03 3.4e-03 4.7e-03 6.2e-03 7.7e-03 9.2e-03 1.1e-02 1.2e-02
10^2 2.1e-03 6.4e-03 1.1e-02 1.5e-02 2.2e-02 3.4e-02 4.7e-02 6.1e-02 7.6e-02 9.1e-02 1.1e-01 1.2e-01
10^1 2.1e-02 6.3e-02 1.0e-01 1.5e-01 2.1e-01 3.2e-01 4.4e-01 5.6e-01 6.8e-01 8.0e-01 9.2e-01 1.0e+00
1 2.1e-01 5.6e-01 8.7e-01 1.1e+00 1.5e+00 1.9e+00 2.2e+00 2.4e+00 2.6e+00 2.7e+00 2.8e+00 2.8e+00
10^{-1} 1.4e+00 2.1e+00 2.0e+00 1.8e+00 1.5e+00 1.2e+00 9.8e-01 8.7e-01 8.0e-01 7.5e-01 7.2e-01 7.1e-01
10^{-2} 1.4e+00 5.9e-01 3.4e-01 2.3e-01 1.4e-01 7.7e-02 4.8e-02 3.3e-02 2.5e-02 2.0e-02 1.7e-02 1.6e-02
0.1 0.3 0.5 0.7 1.0 1.5 2.0 2.5 3.0 3.5 4.0 4.4
m_ϕ (GeV)
10^0
10^{-1}
10^{-2}
10^{-3}
10^{-4}
Acceptance (%)

CODEX-B

CODEX-b(“COmpact Detector for EXotics at LHCb”) is proposed to search for LLPs decaying with $c\tau > 1\,\mathrm{m}$ [10] with an integrated luminosity of $300\,\mathrm{fb}^{-1}$. This detector is to be installed near the LHCb interaction point.

[10] Aielli et al., Arxiv:2203.07316

CODEX-b

CODEX-b(“COmpact Detector for EXotics at LHCb”) is proposed to search for LLPs decaying with $c\tau >$1 m [10] with an integrated luminosity of 300 fb^{-1}. This detector is to be installed near the LHCb interaction point.
The considered dimensions for this detector is a $10 \times 10 \times 10\,\mathrm{m}^3$ decay volume and if possible, a bigger size of $20 \times 10 \times 10\,\mathrm{m}^3$, with the following position:

- **CODEX** – **b** : $26.0\ \mathrm{m} < \mathrm{x} < 46.0\ \mathrm{m}, -7.0\ \mathrm{m} < \mathrm{y} < 3.0\ \mathrm{m}, 5.0\ \mathrm{m} < \mathrm{z} < 15.0\ \mathrm{m}$

[10] Aielli et al., Arxiv:2203.07316

MATHUSLA

`MATHUSLA(“MAssive Timing Hodoscope for Ultra-Stable neutraL pArticles”)` [11] is proposed to detect particle with $c\tau > 100\,\mathrm{m}$ at the 14 TeV HL-LHC with an integrated luminosity of $3ab^{-1}$. MATHUSLA is intended to be positioned near the CMS interaction point at the HL-LHC.

[11] MATHUSLA collaboration, JINST 15 (2020) C06026

MATHUSLA

`MATHUSLA(“MAssive Timing Hodoscope for Ultra-Stable neutraL pArticles”)` [11] is proposed to detect particle with $c\tau > 100\,\mathrm{m}$ at the 14 TeV HL-LHC with an integrated luminosity of $3ab^{-1}$. MATHUSLA is intended to be positioned near the CMS interaction point at the HL-LHC.

- **MATHUSLA** : $60.0\ \mathrm{m} < \mathrm{x} < 85.0\ \mathrm{m}, -50.0\ \mathrm{m} < \mathrm{y} < 50.0\ \mathrm{m}, 68.0\ \mathrm{m} < \mathrm{z} < 168.0\ \mathrm{m}$

[11] MATHUSLA collaboration, JINST 15 (2020) C06026

DELIGHT

DELIGHT(“Detector for long-lived particles at high energy of 100 TeV”) is a transverse detector that is proposed to detect LLPs at the 100 TeV LHC, as discussed in [12].

[12] Bhattacherjee et al., Phys. Rev. D 106 (2022) 095018

DELIGHT

DELIGHT(“Detector for long-lived particles at high energy of 100 TeV”) is a transverse detector that is proposed to detect LLPs at the 100 TeV LHC, as discussed in [12].

- **DELIGHT** – **A** : $25.0\ \mathrm{m} < \mathrm{x} < 50.0\ \mathrm{m}, 0.0\ \mathrm{m} < \mathrm{y} < 100.0\ \mathrm{m}, -50.0\ \mathrm{m} < \mathrm{z} < 50.0\ \mathrm{m}$
- **DELIGHT** – **B** : $25.0\ \mathrm{m} < \mathrm{x} < 125.0\ \mathrm{m}, 0.0\ \mathrm{m} < \mathrm{y} < 100.0\ \mathrm{m}, -50.0\ \mathrm{m} < \mathrm{z} < 50.0\ \mathrm{m}$
- **DELIGHT** – **C** : $25.0\ \mathrm{m} < \mathrm{x} < 225.0\ \mathrm{m}, 0.0\mathrm{m} < \mathrm{y} < 50.0\ \mathrm{m}, -25.0\ \mathrm{m} < \mathrm{z} < 25.0\ \mathrm{m}$

[12] Bhattacherjee et al., Phys. Rev. D 106 (2022) 095018

Comparison

m_ϕ (GeV)	$c\tau$ (m)	FASER2 ($p_\phi > 100$GeV)	CODEX-b ($E_\phi > 1$GeV)	MATHUSLA ($E_\phi > 1$GeV)	FOREHUNT-C ($p_\phi > 100$GeV)	DELIGHT-B ($E_\phi > 1$GeV)
0.1	10^1	$1.6 \times 10^{-5}\%$	$1.0 \times 10^{-2}\%$	$1.3 \times 10^{-1}\%$	$2.1 \times 10^{-2}\%$	$\mathbf{6.5 \times 10^{-1}\%}$
0.1	10^4	$1.5 \times 10^{-8}\%$	$1.1 \times 10^{-5}\%$	$2.1 \times 10^{-4}\%$	$2.1 \times 10^{-5}\%$	$\mathbf{9.2 \times 10^{-4}\%}$
2.0	10^1	$3.6 \times 10^{-4}\%$	$1.8 \times 10^{-2}\%$	$4.4 \times 10^{-2}\%$	$4.4 \times 10^{-1}\%$	$\mathbf{5.3 \times 10^{-1}\%}$
2.0	10^4	$4.8 \times 10^{-7}\%$	$1.9 \times 10^{-4}\%$	$3.4 \times 10^{-3}\%$	$4.7 \times 10^{-4}\%$	$\mathbf{1.5 \times 10^{-2}\%}$
4.4	10^1	$8.6 \times 10^{-4}\%$	$9.2 \times 10^{-3}\%$	$1.3 \times 10^{-2}\%$	$\mathbf{1.0\%}$	$2.5 \times 10^{-1}\%$
4.4	10^4	$1.5 \times 10^{-6}\%$	$2.3 \times 10^{-4}\%$	$5.0\% \times 10^{-3}\%$	$1.2 \times 10^{-3}\%$	$\mathbf{1.9 \times 10^{-2}\%}$

Comparison

m_ϕ (GeV)	cτ (m)	FASER2 ($p_\phi > 100$GeV)	CODEX-b ($E_\phi > 1$GeV)	MATHUSLA ($E_\phi > 1$GeV)	FOREHUNT-C ($p_\phi > 100$GeV)	DELIGHT-B ($E_\phi > 1$GeV)
0.1	10^1	$1.6 \times 10^{-5}\%$	$1.0 \times 10^{-2}\%$	$1.3 \times 10^{-1}\%$	$2.1 \times 10^{-2}\%$	$\mathbf{6.5 \times 10^{-1}\%}$
0.1	10^4	$1.5 \times 10^{-8}\%$	$1.1 \times 10^{-5}\%$	$2.1 \times 10^{-4}\%$	$2.1 \times 10^{-5}\%$	$\mathbf{9.2 \times 10^{-4}\%}$
2.0	10^1	$3.6 \times 10^{-4}\%$	$1.8 \times 10^{-2}\%$	$4.4 \times 10^{-2}\%$	$4.4 \times 10^{-1}\%$	$\mathbf{5.3 \times 10^{-1}\%}$
2.0	10^4	$4.8 \times 10^{-7}\%$	$1.9 \times 10^{-4}\%$	$3.4 \times 10^{-3}\%$	$4.7 \times 10^{-4}\%$	$\mathbf{1.5 \times 10^{-2}\%}$
4.4	10^1	$8.6 \times 10^{-4}\%$	$9.2 \times 10^{-3}\%$	$1.3 \times 10^{-2}\%$	**1.0%**	$2.5 \times 10^{-1}\%$
4.4	10^4	$1.5 \times 10^{-6}\%$	$2.3 \times 10^{-4}\%$	$5.0\% \times 10^{-3}\%$	$1.2 \times 10^{-3}\%$	$\mathbf{1.9 \times 10^{-2}\%}$

DELIGHT performs very well for most of the benchmark points with $c\tau > 10^1$ m.

DELIGHT for Dark-Higgs

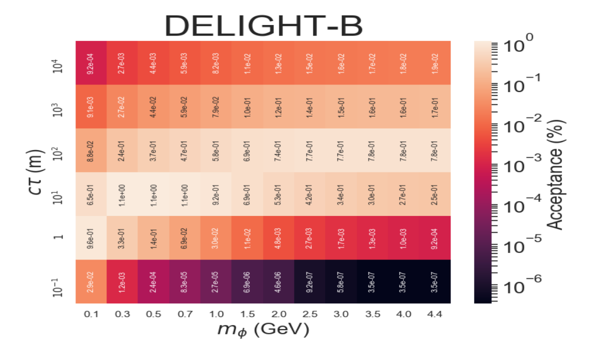

DELIGHT for Dark-Higgs

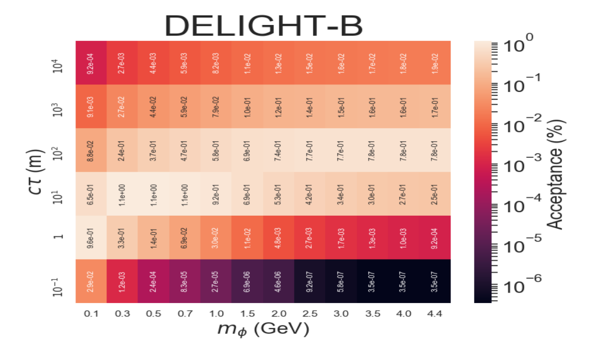

- $m_\phi = 4.4$ GeV and $c\tau = 1$ m, FOREHUNT-C outperforms DELIGHT-B by a factor of $\mathcal{O}(3 \times 10^3)$.
- DELIGHT-B superior performance for decay lengths $\geq 10^2$ m.
- For $c\tau \approx 10$ m, DELIGHT-B performs better than FOREHUNT-C for LLPs with masses < 2.5 GeV.

Final Result

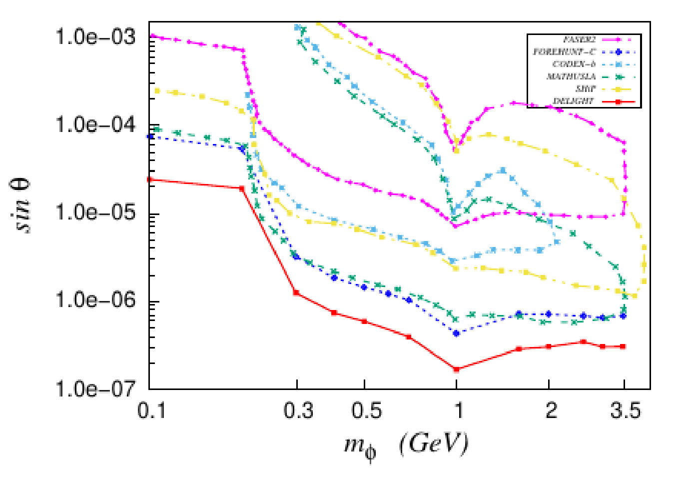

Conclusion

- Detection prospect of light LLPs coming from B-meson decays at the FCC-hh for dark Higgs boson.

Conclusion

- Detection prospect of light LLPs coming from B-meson decays at the FCC-hh for dark Higgs boson.
- Compared to FASER2, enhance the sensitivity by a factor of 20 for the dark Higgs model. $\rightarrow$ **DELIGHT** performs even well.

Conclusion

- Detection prospect of light LLPs coming from B-meson decays at the FCC-hh for dark Higgs boson.
- Compared to FASER2, enhance the sensitivity by a factor of 20 for the dark Higgs model. $\rightarrow$ **DELIGHT** performs even well.
- For model-independent analysis, our analysis reveals that if the LLP has low decay length < 10 m, a forward detector like FOREHUNT is the best option to look for the decaying LLP, while DELIGHT is preferable for higher decay lengths.

Conclusion

- Detection prospect of light LLPs coming from B-meson decays at the FCC-hh for dark Higgs boson.
- Compared to FASER2, enhance the sensitivity by a factor of 20 for the dark Higgs model. $\rightarrow$ **DELIGHT** performs even well.
- For model-independent analysis, our analysis reveals that if the LLP has low decay length < 10 m, a forward detector like FOREHUNT is the best option to look for the decaying LLP, while DELIGHT is preferable for higher decay lengths.

Dark Higgs

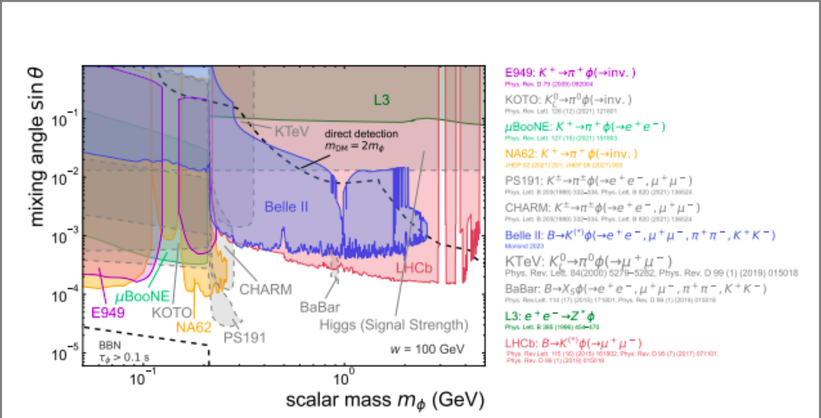

mixing angle sin θ
scalar mass m_ϕ (GeV)
L3
KTeV
direct detection
$m_{DM} = 2m_\phi$
Belle II
LHCb
CHARM
BaBar
Higgs (Signal Strength)
μBooNE
E949
KOTO
NA62
PS191
BBN
$\tau_\phi > 0.1$ s
w = 100 GeV
E949: $K^+ \to \pi^+ \phi(\to \text{inv.})$
KOTO: $K_L^0 \to \pi^0 \phi(\to \text{inv.})$
μBooNE: $K^+ \to \pi^+ \phi(\to e^+ e^-)$
NA62: $K^+ \to \pi^+ \phi(\to \text{inv.})$
PS191: $K^\pm \to \pi^\pm \phi(\to e^+ e^-, \mu^+ \mu^-)$
CHARM: $K^\pm \to \pi^\pm \phi(\to e^+ e^-, \mu^+ \mu^-)$
Belle II: $B \to K^{(*)} \phi(\to e^+ e^-, \mu^+ \mu^-, \pi^+ \pi^-, K^+ K^-)$
KTeV: $K_L^0 \to \pi^0 \phi(\to \mu^+ \mu^-)$
Phys. Rev. Lett. 84(2000) 5279–5282, Phys. Rev. D 99 (1) (2019) 015018
BaBar: $B \to X_S \phi(\to e^+ e^-, \mu^+ \mu^-, \pi^+ \pi^-, K^+ K^-)$
L3: $e^+ e^- \to Z^* \phi$
LHCb: $B \to K^{(*)} \phi(\to \mu^+ \mu^-)$

Dark Higgs

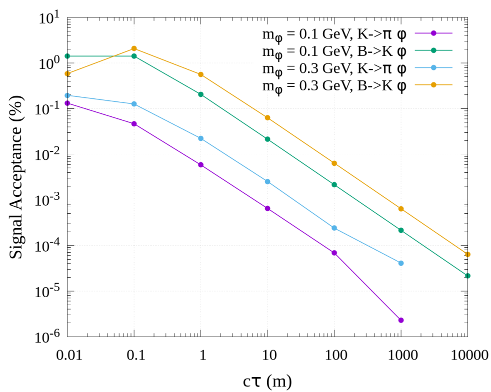

Signal Acceptance (%)
cτ (m)
m_φ = 0.1 GeV, K->π φ
m_φ = 0.1 GeV, B->K φ
m_φ = 0.3 GeV, K->π φ
m_φ = 0.3 GeV, B->K φ
0.01
0.1
1
10
100
1000
10000
10^{1}
10^{0}
10^{-1}
10^{-2}
10^{-3}
10^{-4}
10^{-5}
10^{-6}

Dark Higgs

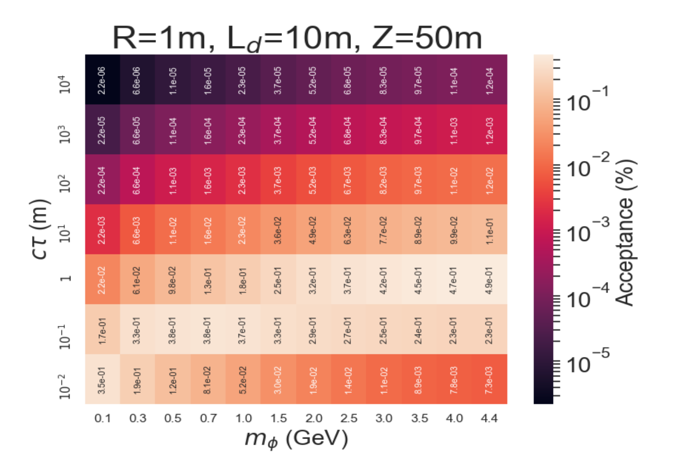
R=1m, L$_d$=10m, Z=50m
$c\tau$ (m)
10^4 10^3 10^2 10^1 1 10^{-1} 10^{-2}
2.2e-06 6.6e-06 1.1e-05 1.6e-05 2.3e-05 3.7e-05 5.2e-05 6.8e-05 8.3e-05 9.7e-05 1.1e-04 1.2e-04
2.2e-05 6.6e-05 1.1e-04 1.6e-04 2.3e-04 3.7e-04 5.2e-04 6.8e-04 8.3e-04 9.7e-04 1.1e-03 1.2e-03
2.2e-04 6.6e-04 1.1e-03 1.6e-03 2.3e-03 3.7e-03 5.2e-03 6.7e-03 8.2e-03 9.7e-03 1.1e-02 1.2e-02
2.2e-03 6.6e-03 1.1e-02 1.6e-02 2.3e-02 3.6e-02 4.9e-02 6.3e-02 7.7e-02 8.9e-02 9.9e-02 1.1e-01
2.2e-02 6.1e-02 9.8e-02 1.3e-01 1.8e-01 2.5e-01 3.2e-01 3.7e-01 4.2e-01 4.5e-01 4.7e-01 4.9e-01
1.7e-01 3.3e-01 3.8e-01 3.8e-01 3.7e-01 3.3e-01 2.9e-01 2.7e-01 2.5e-01 2.4e-01 2.3e-01 2.3e-01
3.5e-01 1.9e-01 1.2e-01 8.1e-02 5.2e-02 3.0e-02 1.9e-02 1.4e-02 1.1e-02 8.9e-03 7.8e-03 7.3e-03
0.1 0.3 0.5 0.7 1.0 1.5 2.0 2.5 3.0 3.5 4.0 4.4
m_ϕ (GeV)
10^{-1} 10^{-2} 10^{-3} 10^{-4} 10^{-5}
Acceptance (%)

Dark Higgs

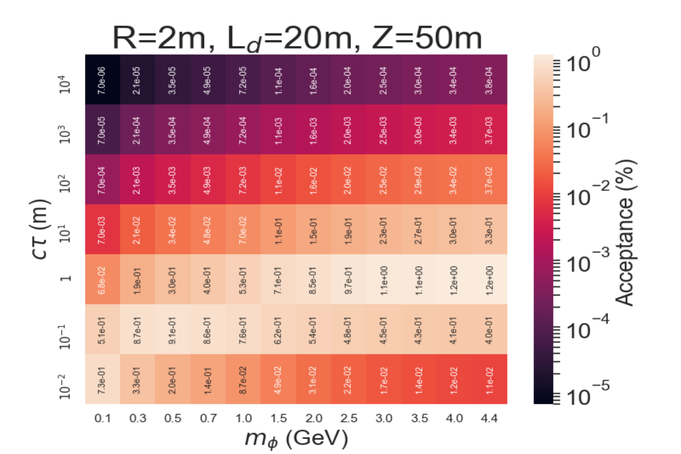
R=2m, L$_d$=20m, Z=50m
cτ (m)
10^4
7.0e-06 2.1e-05 3.5e-05 4.9e-05 7.2e-05 1.1e-04 1.6e-04 2.0e-04 2.5e-04 3.0e-04 3.4e-04 3.8e-04
10^3
7.0e-05 2.1e-04 3.5e-04 4.9e-04 7.2e-04 1.1e-03 1.6e-03 2.0e-03 2.5e-03 3.0e-03 3.4e-03 3.7e-03
10^2
7.0e-04 2.1e-03 3.5e-03 4.9e-03 7.2e-03 1.1e-02 1.6e-02 2.0e-02 2.5e-02 2.9e-02 3.4e-02 3.7e-02
10^1
7.0e-03 2.1e-02 3.4e-02 4.8e-02 7.0e-02 1.1e-01 1.5e-01 1.9e-01 2.3e-01 2.7e-01 3.0e-01 3.3e-01
1
6.8e-02 1.9e-01 3.0e-01 4.0e-01 5.3e-01 7.1e-01 8.5e-01 9.7e-01 1.1e+00 1.1e+00 1.2e+00 1.2e+00
10^{-1}
5.1e-01 8.7e-01 9.1e-01 8.6e-01 7.6e-01 6.2e-01 5.4e-01 4.8e-01 4.5e-01 4.3e-01 4.1e-01 4.0e-01
10^{-2}
7.3e-01 3.3e-01 2.0e-01 1.4e-01 8.7e-02 4.9e-02 3.1e-02 2.2e-02 1.7e-02 1.4e-02 1.2e-02 1.1e-02
0.1 0.3 0.5 0.7 1.0 1.5 2.0 2.5 3.0 3.5 4.0 4.4
m_ϕ (GeV)
10^0 10^{-1} 10^{-2} 10^{-3} 10^{-4} 10^{-5}
Acceptance (%)

Dark Higgs

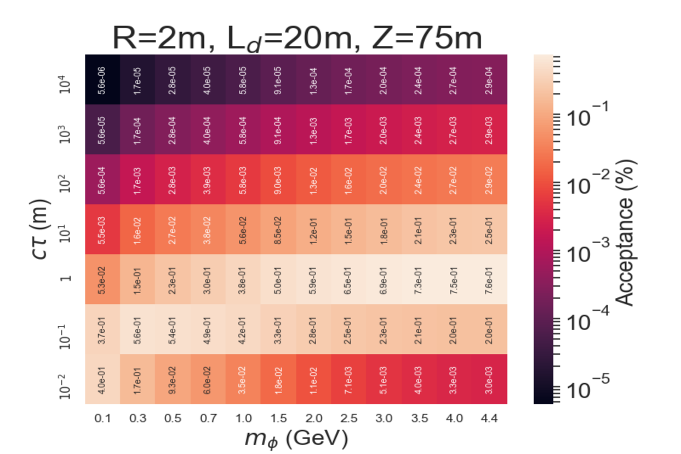
R=2m, L$_d$=20m, Z=75m
10^4 5.6e-06 1.7e-05 2.8e-05 4.0e-05 5.8e-05 9.1e-05 1.3e-04 1.7e-04 2.0e-04 2.4e-04 2.7e-04 2.9e-04
10^3 5.6e-05 1.7e-04 2.8e-04 4.0e-04 5.8e-04 9.1e-04 1.3e-03 1.7e-03 2.0e-03 2.4e-03 2.7e-03 2.9e-03
10^2 5.6e-04 1.7e-03 2.8e-03 3.9e-03 5.8e-03 9.0e-03 1.3e-02 1.6e-02 2.0e-02 2.4e-02 2.7e-02 2.9e-02
10^1 5.5e-03 1.6e-02 2.7e-02 3.8e-02 5.6e-02 8.5e-02 1.2e-01 1.5e-01 1.8e-01 2.1e-01 2.3e-01 2.5e-01
1 5.3e-02 1.5e-01 2.3e-01 3.0e-01 3.8e-01 5.0e-01 5.9e-01 6.5e-01 6.9e-01 7.3e-01 7.5e-01 7.6e-01
10^{-1} 3.7e-01 5.6e-01 5.4e-01 4.9e-01 4.2e-01 3.3e-01 2.8e-01 2.5e-01 2.3e-01 2.1e-01 2.0e-01 2.0e-01
10^{-2} 4.0e-01 1.7e-01 9.3e-02 6.0e-02 3.5e-02 1.8e-02 1.1e-02 7.1e-03 5.1e-03 4.0e-03 3.3e-03 3.0e-03
$c\tau$ (m)
0.1 0.3 0.5 0.7 1.0 1.5 2.0 2.5 3.0 3.5 4.0 4.4
m_ϕ (GeV)
10^{-1} 10^{-2} 10^{-3} 10^{-4} 10^{-5}
Acceptance (%)

Dark Higgs

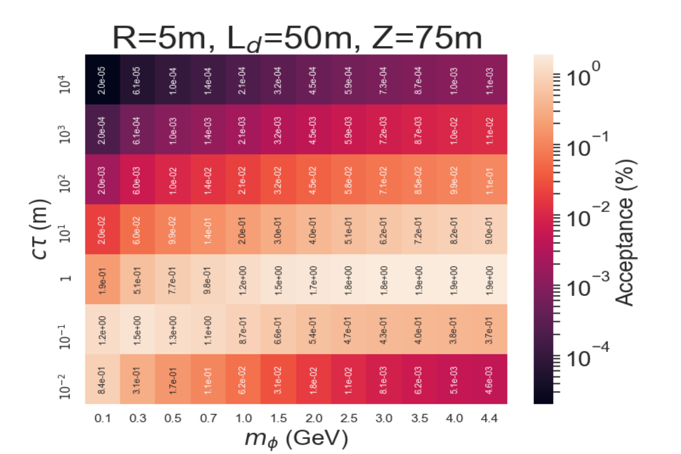
R=5m, L_d=50m, Z=75m
$c\tau$ (m)
10^4
2.0e-05 6.1e-05 1.0e-04 1.4e-04 2.1e-04 3.2e-04 4.5e-04 5.9e-04 7.3e-04 8.7e-04 1.0e-03 1.1e-03
10^3
2.0e-04 6.1e-04 1.0e-03 1.4e-03 2.1e-03 3.2e-03 4.5e-03 5.9e-03 7.2e-03 8.7e-03 1.0e-02 1.1e-02
10^2
2.0e-03 6.0e-03 1.0e-02 1.4e-02 2.1e-02 3.2e-02 4.5e-02 5.8e-02 7.1e-02 8.5e-02 9.9e-02 1.1e-01
10^1
2.0e-02 6.0e-02 9.9e-02 1.4e-01 2.0e-01 3.0e-01 4.0e-01 5.1e-01 6.2e-01 7.2e-01 8.2e-01 9.0e-01
1
1.9e-01 5.1e-01 7.7e-01 9.8e-01 1.2e+00 1.5e+00 1.7e+00 1.8e+00 1.8e+00 1.9e+00 1.9e+00 1.9e+00
10^{-1}
1.2e+00 1.5e+00 1.3e+00 1.1e+00 8.7e-01 6.6e-01 5.4e-01 4.7e-01 4.3e-01 4.0e-01 3.8e-01 3.7e-01
10^{-2}
8.4e-01 3.1e-01 1.7e-01 1.1e-01 6.2e-02 3.1e-02 1.8e-02 1.1e-02 8.1e-03 6.2e-03 5.1e-03 4.6e-03
0.1 0.3 0.5 0.7 1.0 1.5 2.0 2.5 3.0 3.5 4.0 4.4
m_ϕ (GeV)
10^0
10^{-1}
10^{-2}
10^{-3}
10^{-4}
Acceptance (%)

Dark Higgs

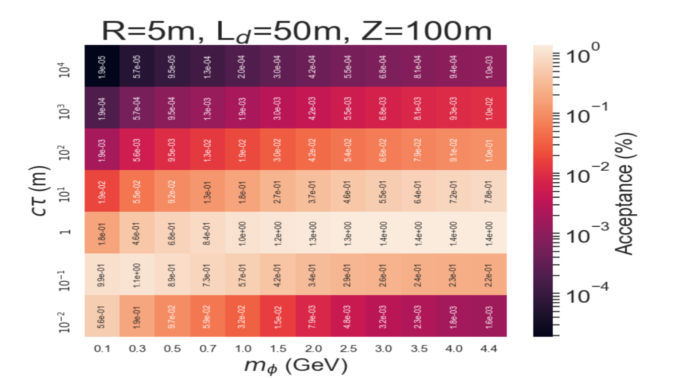
R=5m, L_d=50m, Z=100m
cτ (m)
10^4
1.9e-05 5.7e-05 9.5e-05 1.3e-04 2.0e-04 3.0e-04 4.2e-04 5.5e-04 6.8e-04 8.1e-04 9.4e-04 1.0e-03
10^3
1.9e-04 5.7e-04 9.5e-04 1.3e-03 1.9e-03 3.0e-03 4.2e-03 5.5e-03 6.8e-03 8.1e-03 9.3e-03 1.0e-02
10^2
1.9e-03 5.6e-03 9.5e-03 1.3e-02 1.9e-02 3.0e-02 4.2e-02 5.4e-02 6.6e-02 7.9e-02 9.1e-02 1.0e-01
10^1
1.9e-02 5.5e-02 9.2e-02 1.3e-01 1.8e-01 2.7e-01 3.7e-01 4.6e-01 5.5e-01 6.4e-01 7.2e-01 7.8e-01
1
1.8e-01 4.6e-01 6.8e-01 8.4e-01 1.0e+00 1.2e+00 1.3e+00 1.3e+00 1.4e+00 1.4e+00 1.4e+00 1.4e+00
10^-1
9.9e-01 1.1e+00 8.9e-01 7.3e-01 5.7e-01 4.2e-01 3.4e-01 2.9e-01 2.6e-01 2.4e-01 2.3e-01 2.2e-01
10^-2
5.6e-01 1.9e-01 9.7e-02 5.9e-02 3.2e-02 1.5e-02 7.9e-03 4.8e-03 3.2e-03 2.3e-03 1.8e-03 1.6e-03
0.1 0.3 0.5 0.7 1.0 1.5 2.0 2.5 3.0 3.5 4.0 4.4
m_ϕ (GeV)
10^0
10^-1
10^-2
10^-3
10^-4
Acceptance (%)

m_ϕ (GeV)	$c\tau$ (m)	acceptance for first detector at z=50 m	acceptance for second detector at z=100 (150) m	acceptance for second detector at z=300 m
0.1	10^{-1}	1.4×10^{-2}	9.9×10^{-3} (7.0×10^{-3})	2.9×10^{-3}
4.4	10^{-1}	7.0×10^{-3}	2.2×10^{-3} (1.0×10^{-3})	1.9×10^{-4}
0.1	10^{4}	2.1×10^{-7}	1.9×10^{-7} (1.6×10^{-7})	9.3×10^{-8}
4.4	10^{4}	1.2×10^{-5}	1.0×10^{-5} (8.5×10^{-6})	4.9×10^{-6}

m_ϕ (GeV)	$c\tau$ (m)	acceptance for first detector at z=50 m	acceptance for second detector at z=100 (150) m	acceptance for second detector at z=300 m
0.1	10^{-1}	1.4×10^{-2}	9.9×10^{-3} (7.0×10^{-3})	2.9×10^{-3}
4.4	10^{-1}	7.0×10^{-3}	2.2×10^{-3} (1.0×10^{-3})	1.9×10^{-4}
0.1	10^{4}	2.1×10^{-7}	1.9×10^{-7} (1.6×10^{-7})	9.3×10^{-8}
4.4	10^{4}	1.2×10^{-5}	1.0×10^{-5} (8.5×10^{-6})	4.9×10^{-6}

m_ϕ (GeV)	$c\tau$ (m)	1 m off-axis ($p_\phi > 100$ GeV)	5 m off-axis ($p_\phi > 100$ GeV)
0.1	10^{-1}	0.83%	5.5×10^{-2}%
4.4	10^{-1}	1.53×10^{-2}%	1.2×10^{-4}%
0.1	10^{4}	1.5×10^{-5}%	8.7×10^{-7}%
4.4	10^{4}	8.4×10^{-4}%	1.7×10^{-4}%

m_ϕ (GeV)	$c\tau$ (m)	FOREHUNT-C ($p_\phi > 50$ GeV, z=100 m)	FOREHUNT-C ($p_\phi > 50$ GeV, z=200 m)	FOREHUNT-C ($p_\phi > 50$ GeV, z=300 m)
0.1	10^{1}	3.3×10^{-2}%	1.8×10^{-2}%	1.1×10^{-2}%
0.1	10^{4}	3.3×10^{-5}%	1.8×10^{-5}%	1.2×10^{-5}%
2.0	10^{1}	6.0×10^{-1}%	3.0×10^{-1}%	2.0×10^{-1}%
2.0	10^{4}	7.4×10^{-4}%	4.4×10^{-4}%	3.0×10^{-4}%
4.4	10^{1}	1.1%	5.0×10^{-1}%	3.0×10^{-1}%
4.4	10^{4}	1.6×10^{-3}%	9.0×10^{-4}%	5.9×10^{-4}%

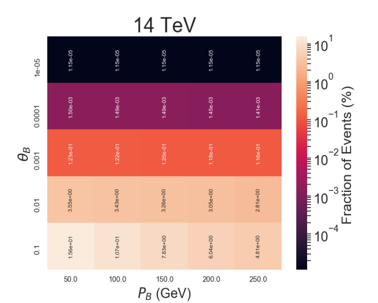
14 TeV
θ_B
1e-05
0.0001
0.001
0.01
0.1
1.15e-05 1.15e-05 1.15e-05 1.15e-05 1.15e-05
1.50e-03 1.49e-03 1.49e-03 1.45e-03 1.41e-03
1.23e-01 1.22e-01 1.20e-01 1.18e-01 1.16e-01
3.55e+00 3.43e+00 3.26e+00 3.05e+00 2.81e+00
1.56e+01 1.07e+01 7.83e+00 6.04e+00 4.81e+00
50.0
100.0
150.0
200.0
250.0
P_B (GeV)
10^1
10^0
10^{-1}
10^{-2}
10^{-3}
10^{-4}
Fraction of Events (%)

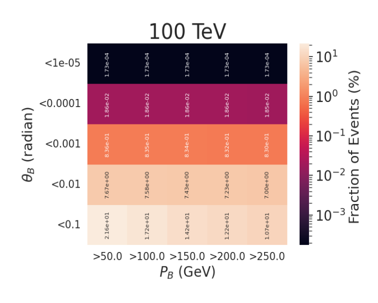
100 TeV
θ_B (radian)
<1e-05
<0.0001
<0.001
<0.01
<0.1
1.73e-04 1.73e-04 1.73e-04 1.73e-04 1.73e-04
1.86e-02 1.86e-02 1.86e-02 1.86e-02 1.85e-02
8.36e-01 8.35e-01 8.34e-01 8.32e-01 8.30e-01
7.67e+00 7.58e+00 7.43e+00 7.23e+00 7.00e+00
2.16e+01 1.72e+01 1.42e+01 1.22e+01 1.07e+01
>50.0
>100.0
>150.0
>200.0
>250.0
P_B (GeV)
10^1
10^0
10^{-1}
10^{-2}
10^{-3}
Fraction of Events (%)

Cost Estimation

- The typical cost of BIS78 RPCs are around 3.1 k€/m^2 [13].
- We propose to place several circular layers of RPCs transverse to the length of the cylindrical decay volume.
- For FOREHUNT-C, the estimated cost per layer of RPC would be around 245 k€.

[13] Bauer et al., Arxiv:1909.13022